

Supporting Information

pH induced dual "OFF-ON-OFF" switch: influence of suitably placed carboxylic acid

Kalyan K. Sadhu, Shin Mizukami, Akimasa Yoshimura, and Kazuya Kikuchi*

Division of Advanced Science and Biotechnology, Graduate School of Engineering, and Immunology Frontier Research Center Osaka University,
2-1 Yamadaoka, Suita, Osaka 565-0871, Japan

* To whom correspondence should be addressed: kkikuchi@mls.eng.osaka-u.ac.jp

CONTENTS:

| | |
|----------------------------------|---------|
| 1. Materials and Instruments | SI2 |
| 2. Experimental Procedures | SI2 |
| 3. Supporting Figures and Tables | SI3-SI8 |
| 4. Supporting References | SI8 |

1. Materials and Instruments

General Chemicals for organic synthesis were of the best grade available, supplied by Tokyo Chemical Industries, Wako Pure Chemical, Aldrich Chemical Co, and were used without further purification.

NMR spectra were recorded on a JEOL JNM-AL400 instrument at 400 MHz for ^1H and at 100.4 MHz for ^{13}C NMR, using tetramethylsilane as an internal standard. Mass spectra were measured on a JEOL JMS-700 for FAB. UV-Visible absorbance spectra were measured using a Shimadzu UV1650PC spectrometer. Fluorescence spectra were measured using a Hitachi F4500 spectrometer. Slit width was 5.0 nm for both excitation and emission, and the photomultiplier voltage was 700 V. Fluorescence microscopic images were recorded using a confocal laser scanning microscope (Olympus, FLUOVIEW FV10i) equipped with a $\times 60$ lens and the appropriate emission filters for coumarin and fluorescein probes. The excitation wavelength was 405 nm for **ONNH** probe. The emission filter set used was 420–520 nm for **ONNH** probe. FV10-ASW2.1 imaging software (Olympus) was used for imaging and data analysis. Time-resolved fluorescence decays were recorded in a time-correlated single photon counting (TCSPC) system from HORIBA Jobin Yvon IBH TemPro Fluorescence Lifetime System, with $\lambda_{\text{ex}} = 370$ nm and $\lambda_{\text{em}} = 470, 480$ nm. Data analysis was performed with IBH DAS6 software.

2. Experimental Procedures

HPLC Analysis. Preparative HPLC was performed with an Inertsil ODS-3 (10.0 mm \times 250 mm) column (GL Sciences Inc.) using an HPLC system that comprised a pump (PU-2087, JASCO) and a detector (UV-2075, JASCO).

Fluorescence quantum yield. The fluorescent probe was dissolved in DMSO to obtain 10 mM stock solution; this solution was then diluted to the desired final concentrations by using an appropriate buffer. The fluorescence quantum yield of the probe was estimated in 100 mM sodium phosphate buffer at different pH (Figure S11), using a fluorescence standard, quinine bisulfate in 50 mM H_2SO_4 ($\phi = 0.55$)^{S1} as a reference for comparison.

Fluorescence Life-time. The fluorescence decay of the probe for life time measurement was estimated in 100 mM sodium phosphate at different pH using TCSPC system from HORIBA Jobin Yvon IBH TemPro Fluorescence Lifetime System, with $\lambda_{\text{ex}} = 370$ nm and $\lambda_{\text{em}} = 470, 480$ nm. Data analysis was performed with IBH DAS6 software. The decay time data were analyzed using a sum exponential, employing a nonlinear least-squares deconvolution analysis.^[S2] Average fluorescence lifetimes were calculated as $\sum B_i \tau_i$ with normalized B_i . The radiative and nonradiative decay rate constants are calculated according to the equations available in literature.^[S3]

Fluorescence image with **ONNH.** HEK293T cells maintained in 10% FBS in DMEM (Invitrogen) at 37 °C under 5% CO_2 were washed three times with PBS and incubated with 10 μM **ONNH** for 15 min in different pH buffers at room temperature. The extracellular pH buffer contained 20 mM MOPS or HEPES for adjusting the buffer pH between 6.5 and 8.0. After the culture medium was replaced, microscopic images were acquired. FV10-ASW2.1 imaging software (Olympus) was used for imaging and data analysis.

3. Supporting Figures

(b)

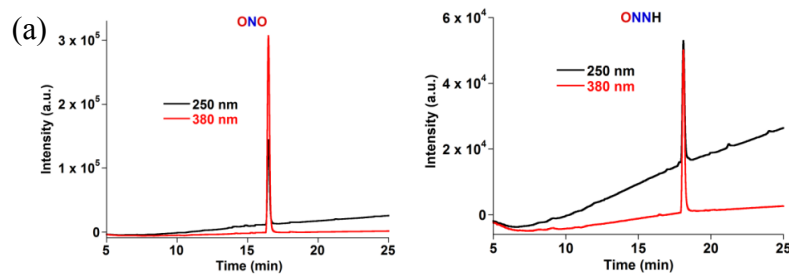


Figure S1. Analytical HPLC data of ONO (a) and ONNH (b) for purity assay with the following eluent condition

| Time (min) | Percentage of eluent A | Percentage of eluent B |
|------------|------------------------|------------------------|
| 0 | 90 | 10 |
| 25 | 10 | 90 |

eluent A: 0.1% formic acid in water

eluent B: 0.1% formic acid in acetonitrile

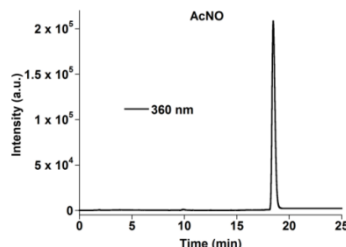


Figure S2. Analytical HPLC data of AcNO for purity assay with the following eluent condition

| Time (min) | Percentage of eluent A | Percentage of eluent B |
|------------|------------------------|------------------------|
| 0 | 50 | 50 |
| 25 | 40 | 60 |

eluent A: 0.1% formic acid in water

eluent B: 0.1% formic acid in acetonitrile

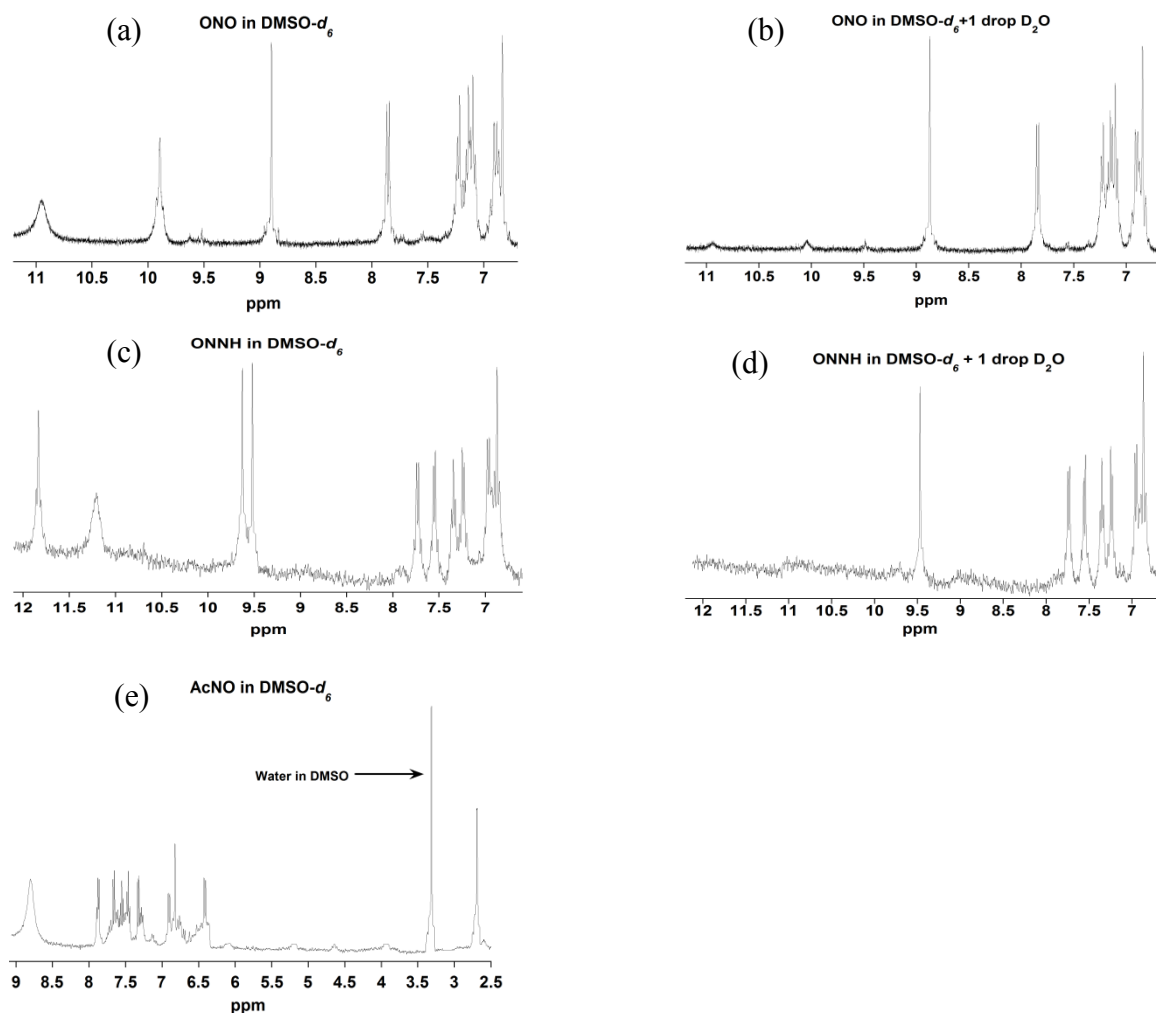


Figure S3. ¹H-NMR spectra of **ONO** (a,b), **ONNH** (c,d) and **AcNO** (e).

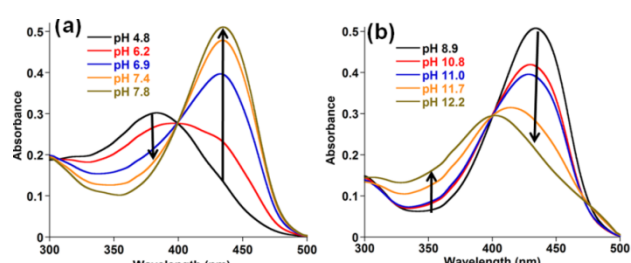


Figure S4. Absorption spectra of 10 μM **ONNH** were measured in 100 mM sodium phosphate buffer containing 1% DMSO at various pH values (a) pH 4.8–7.8 and (b) 8.9–12.2.

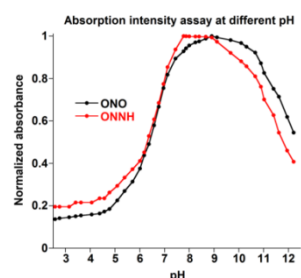


Figure S5. Normalized absorbance of **ONO** and **ONNH** at 415 nm and 435 nm respectively in 100 mM sodium phosphate buffer of various pH containing 1% DMSO at 25 °C.

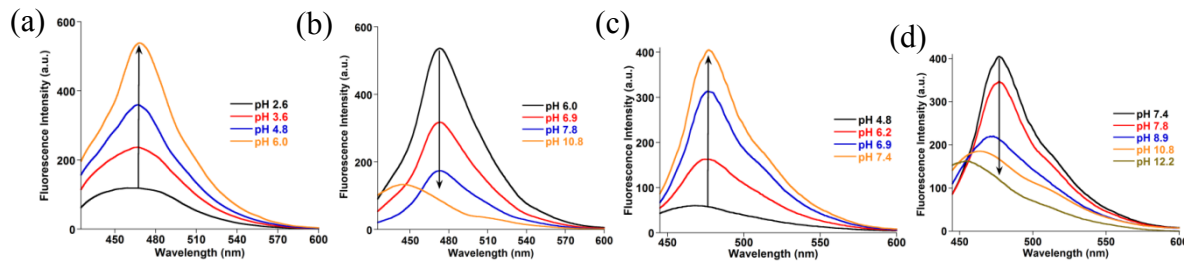


Figure S6. Emission spectra of 1 μM ONO ($\lambda_{\text{ex}} = 415 \text{ nm}$) (a, b) and 1 μM ONNH ($\lambda_{\text{ex}} = 435 \text{ nm}$) (c, d) were measured in 100 mM sodium phosphate buffer containing 0.1% DMSO at different pH values.

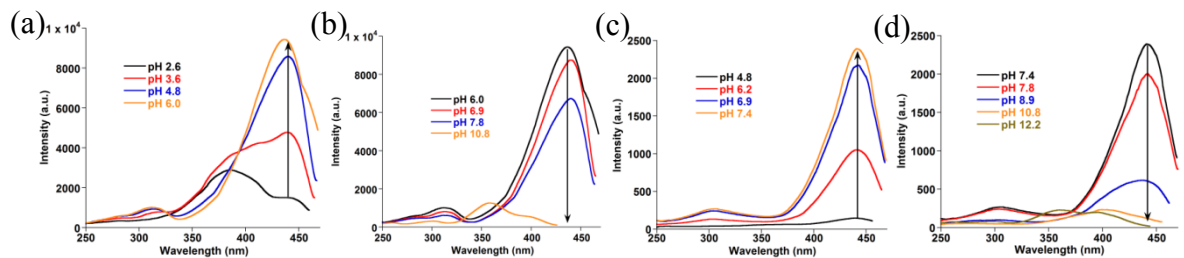


Figure S7. Excitation spectra of 1 μM ONO ($\lambda_{\text{em}} = 470 \text{ nm}$) (a, b) and 1 μM ONNH ($\lambda_{\text{em}} = 480 \text{ nm}$) (c, d) were measured in 100 mM sodium phosphate buffer containing 0.1% DMSO at different pH values.

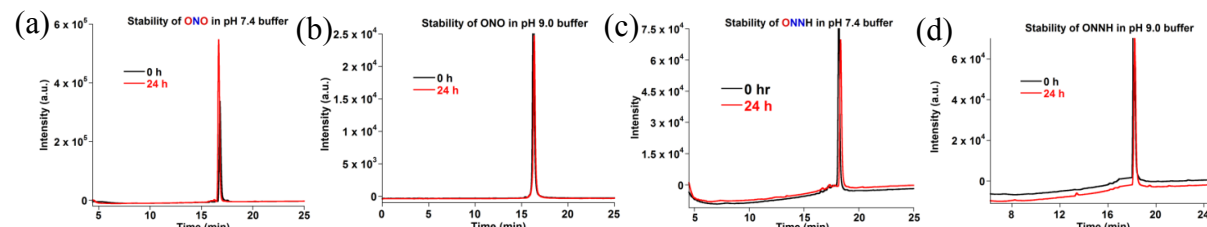


Figure S8. Analytical HPLC data of ONO (a, b) and ONNH (c, d) for 24 h stability at pH 7.4 (a, c) and 9.0 (b, d).

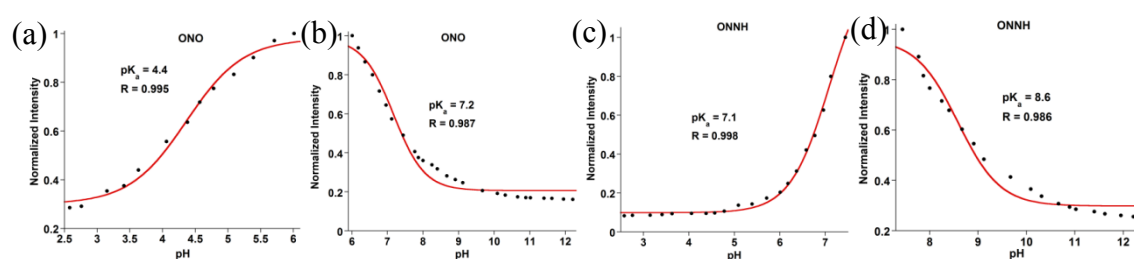


Figure S9. Calculation of $\text{p}K_1^*$ and $\text{p}K_2^*$ of ONO (a, b) and ONNH (c, d) probe based on relative fluorescence assay.

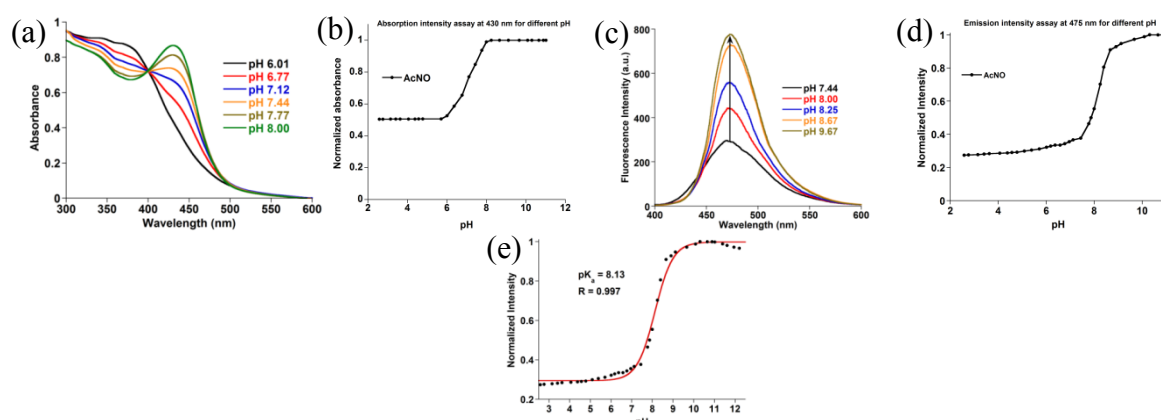


Figure S10. Absorption spectra of 10 μM AcNO (a) with pH profile for absorbance at 430 nm (b), emission spectra of 1 μM AcNO ($\lambda_{\text{ex}} = 430 \text{ nm}$) (c) with pH profile for absorbance at 475 nm (d) and calculation of pK_a^* (e) measured in 100 mM sodium phosphate buffer containing 1% DMSO.

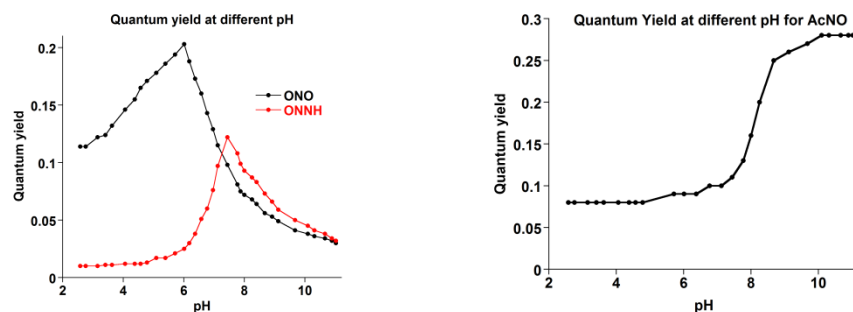


Figure S11. Quantum yield vs. pH plots for ONO, ONNH (left) and AcNO (right).

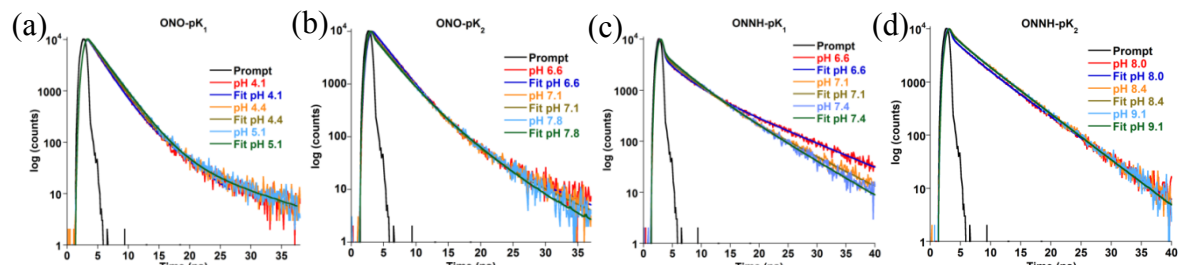


Figure S12. Time-resolved fluorescence decay analysis of ONO (a, b) and ONNH (c, d) at 470 nm in 100 mM sodium phosphate buffer containing 1% DMSO at different pH.

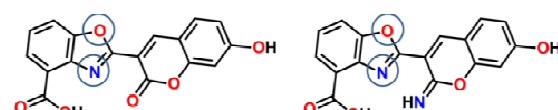


Table S1. Calculated charge on the heteroatoms of the benzoxazolyl parts (marked in the above figure) in ONO and ONNH probes.

| | Charge on N atom | | | Charge on O atom | | |
|-------------|------------------|-----------|---------|------------------|-----------|---------|
| | Neutral | monoanion | dianion | Neutral | monoanion | dianion |
| ONO | -0.177 | -0.251 | -0.037 | -0.481 | -0.505 | -0.498 |
| ONNH | -0.200 | -0.312 | -0.080 | -0.552 | -0.575 | -0.566 |

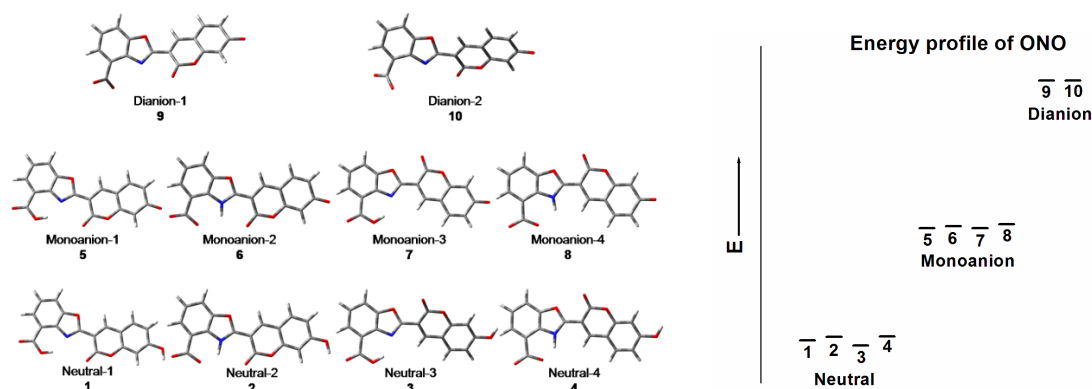


Figure S13. Different energy minimized geometries of **ONO** in the neutral, monoanionic and dianionic forms (left) and their relative energy profile (right).

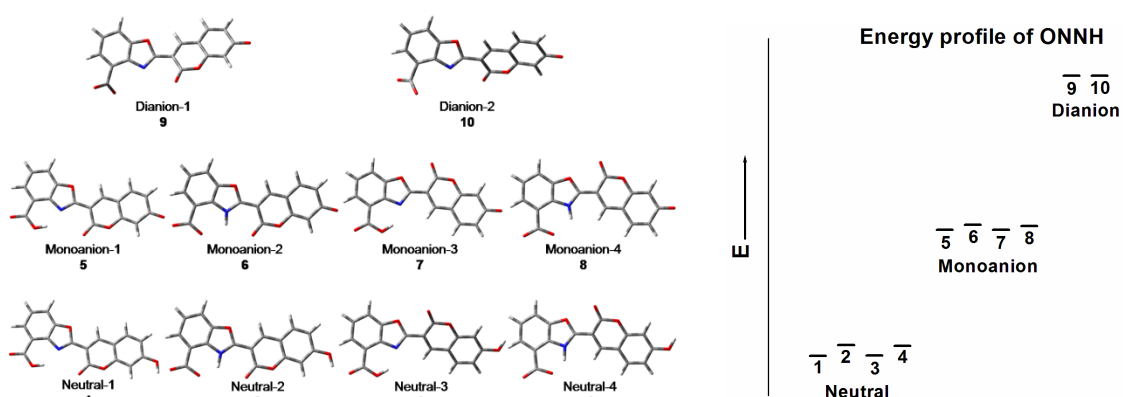


Figure S14. Different energy minimized geometries of **ONNH** in the neutral, monoanionic and dianionic forms (left) and their relative energy profile (right).

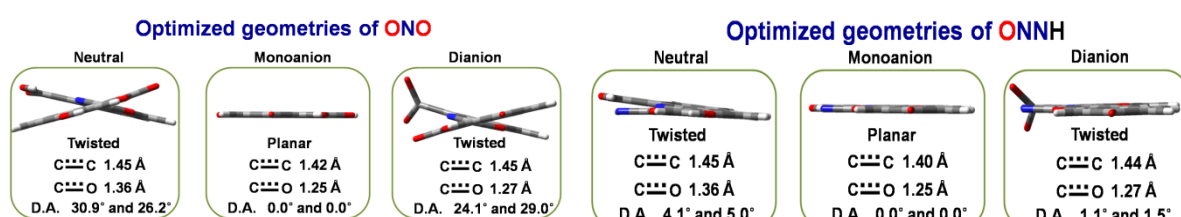


Figure S15. The energy-minimized ground state geometries of **ONO** (geometries 3, 7, 10 Fig. S13) and **ONNH** (geometries 1, 5, 9 Fig. S14) at neutral, monoanion, and dianionic forms along with the dihedral angle (D.A.).

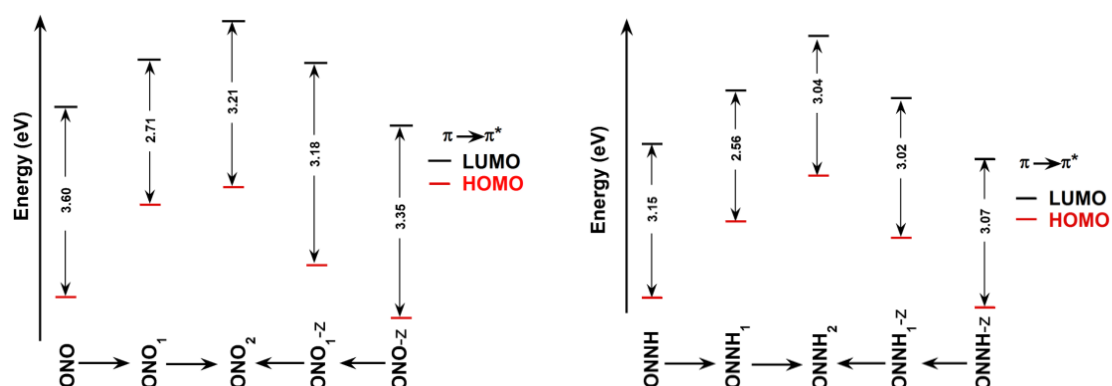


Figure S16. TD-DFT calculated energy gaps for electronic transition in different geometries of **ONO** (left) and **ONNH** (right) in neutral, monoanionic and dianionic forms.

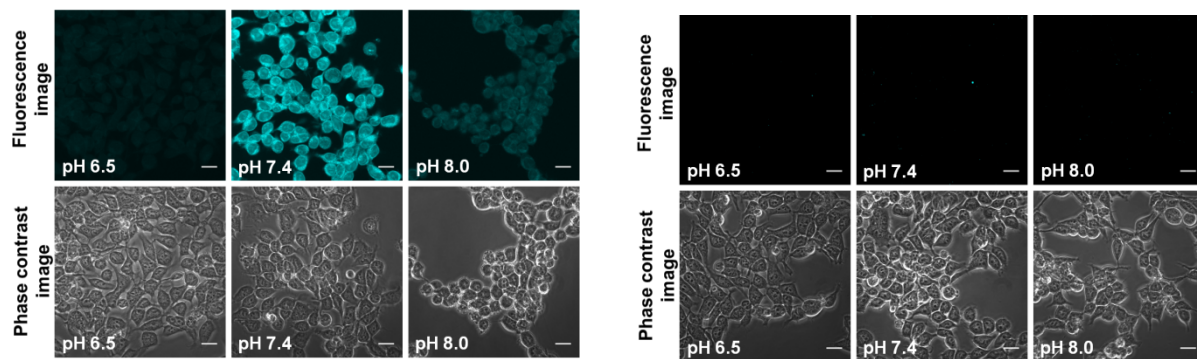


Figure S17. Optical microscopic images of ONNH-labeled HEK293T cells (left) and the control experiment without probes (right) in different pH 6.5, 7.4, and 8.0 at 37 °C. For fluorescence microscopic images, the cells were excited by 405 nm laser lights for each probe.

Complete reference of reference no. 21 of the main text.

M. J. Frisch, G. W. Trucks, H. B. Schlegel, G. E. Scuseria, M. A. Robb, J. R. Cheeseman, G. Scalmani, V. Barone, B. Mennucci, G. A. Petersson, H. Nakatsuji, M. Caricato, X. Li, H. P. Hratchian, A. F. Izmaylov, J. Bloino, G. Zheng, J. L. Sonnenberg, M. Hada, M. Ehara, K. Toyota, R. Fukuda, J. Hasegawa, M. Ishida, T. Nakajima, Y. Honda, O. Kitao, H. Nakai, T. Vreven, J. A. Montgomery, Jr., J. E. Peralta, F. Ogliaro, M. Bearpark, J. J. Heyd, E. Brothers, K. N. Kudin, V. N. Staroverov, R. Kobayashi, J. Normand, K. Raghavachari, A. Rendell, J. C. Burant, S. S. Iyengar, J. Tomasi, M. Cossi, N. Rega, J. M. Millam, M. Klene, J. E. Knox, J. B. Cross, V. Bakken, C. Adamo, J. Jaramillo, R. Gomperts, R. E. Stratmann, O. Yazyev, A. J. Austin, R. Cammi, C. Pomelli, J. W. Ochterski, R. L. Martin, K. Morokuma, V. G. Zakrzewski, G. A. Voth, P. Salvador, J. J. Dannenberg, S. Dapprich, A. D. Daniels, O. Farkas, J. B. Foresman, J. V. Ortiz, J. Cioslowski, and D. J. Fox, Gaussian 09, Revision A.02, Gaussian, Inc., Wallingford, CT, USA, 2009.

4. Supporting References

- S1. R. W. Dawson and W. M. Windsor, *J. Phys. Chem.*, 1968, **72**, 3251.
- S2. G. Hungerford, A. Allison, D. McLoskey, M. K. Kuimova, G. Yahiroglu, K. Suhling, *J. Phys. Chem. B* 2009, **113**, 12067–12074.
- S3. J. R. Lakowicz, *Principles of Fluorescence Spectroscopy*, 3rd ed. Springer Science + Business Media, LLC, 2006.